Content based Computational Chromatic Adaptation

Fatma Kerouh[1,2], Djemel Ziou[3] and Nabil Lahmar[3]
[1]*Institute of Electrical and Electronic Engineering, M'Hamed BOUGARA University, Boumerdes, Algeria*
[2]*USTHB, Image Processing and Radiation Laboratory, Algiers, Algeria*
[3]*Département d'Informatique, Université de Sherbrooke, Sherbrooke, Qc., J1K 2R1, Canada*

Keywords: Computational Chromatic Adaptation, von Kries Transform, Bradford Transform, Sharp Transform, Spatial Content.

Abstract: Chromatic adaptation is needed to accurately reproduce the color appearance of an image. Imaging systems have to apply a transform to convert a color of an image captured under an input illuminant to another output illuminant. This transform is called Chromatic Adaptation Transform (CAT). Different CATs have been proposed in the literature such as von Kries, Bradford and Sharp. Both these transforms consider the adjustment of all the image spatial contents (edges, texture and homogeneous area) in the same way. Our intuition is that, CATs behave differently on the image spatial content. To verify that, we prospect to study the well known CATs effect on the image spatial content, according to some objective criteria. Based on observations we made, a new CAT is derived considering the image spatial content. To achieve that, suitable requirements for CAT are revised and re-written in a variational formalism. Encouraging results are obtained while comparing the proposed CAT to some known ones.

1 INTRODUCTION

The Human Visual System (HVS) has the particularity of dynamically adapting to the changing of light conditions. In fact, HVS is able to carry out automatically a chromatic adaptation in order to preserve color constancy. However, imaging systems as scanners and digital camera have not the ability to adjust their sensors relative response as the HVS. In this case, a transform is needed. It is called Chromatic Adaptation Transform (CAT). Computational color adaptation refers to the use of algorithms to predict the real color of an object when it is seen and captured under different light sources. It is a basic operation in the color appearance model (Fairchild, 2005) (Madin and Ziou, 2014), where the goal is to provide complete and faithful color information that fulfils the requirements of real world applications including, white balance (Wilkie and Weidlich, 2009), (Laine and Saarelma, 2000), (Lee and Goodwin, 1997), (Hirakawa and Parks, 2005), (Spitzer and Semo, 2002), color reproduction (Fairchild, 2005), and color based skin recognition (Bourbakis et al., 2007). Assuming the light sources known, a deterministic prediction is possible if the image formation model allows to write an output image as a function of an input image. According to the von Kries chromatic adaptation theory (Kries, 1970), a color prediction of an object is reached by independently scaling each sensor output value by the output to input ratio in the RGB color space. The implementation is straightforward. The output image is obtained by multiplying the input image and the diagonal matrix of ratios

$$\begin{pmatrix} X' \\ Y' \\ Z' \end{pmatrix} = M^{-1} \begin{pmatrix} \alpha & 0 & 0 \\ 0 & \beta & 0 \\ 0 & 0 & \gamma \end{pmatrix} M \begin{pmatrix} X \\ Y \\ Z \end{pmatrix} \quad (1)$$

A linear CAT can be written as $M^{-1}DM$, (equation (1)), where M is a matrix related to the used color space and D stands for the von Kries transform. Any CAT can be seen as a linear transform of a color space to another one of the same dimension. Where, the columns of M are the basis of the color space and D is a diagonal matrix specifying colors dispersion according to each element of the basis. Given the input color space and the von Kries transform, another issue concerns the choice of the output color space. In some previous works, the space is obtained experimentally by color matching paradigms where the criteria to choose the color space are implicit. However,

Kerouh, F., Ziou, D. and Lahmar, N.
Content based Computational Chromatic Adaptation.
DOI: 10.5220/0005678100390047
In *Proceedings of the 11th Joint Conference on Computer Vision, Imaging and Computer Graphics Theory and Applications (VISIGRAPP 2016) - Volume 2: IVAPP*, pages 41-49
ISBN: 978-989-758-175-5

some criteria were established. According to Lam (Lam, 1985), the CAT should maintain constancy for all neutrals, work with different adapting illuminant, and it should be reversible. More theoretical studies were conducted to identify the requirements to select the suitable color space for color prediction (Gortler et al., 2007; West and Brill., 1982). Among these requirements, narrowing the sensor spectral sensitivity leads to more accurate color prediction. Based on these findings, Finlayson *et al* proposed the Sharp transform (Finlayson et al., 1994). A quantitative evaluation and comparison between some existing transforms can be found in (Luo, 2000; Holm et al., 2010; Bianco and Schettini, 2010). According to these evaluations, the Bradford, Bartleson, Sharp, and CMCCAT2000 transforms perform better than many others. Note that the experimental data set used to derive the transform is another issue. The available data sets are chosen according to some protocols and viewing conditions to reflect realistic situations (Luo, 2000). However, the image content effect on color prediction is not understood because in most previous works the whole data are transformed into XYZ color space coordinates and used to derive a CAT. To summarize, four research area can be discussed in the color adaptation field. The first one concerns the best color space used to implement a CAT. The second issue is about the used transform to adapt the image color appearance. The third one refers to the choice of the best output color space and the last research area concerns the experimental datasets. The purpose of this work falls under the second research area. Our aim is to propose a new color adaptation transform that fulfils some particular requirements.

The image content refers to spatial information such as edges and textures at low abstraction level and to events such as objects, their relationships and context at high abstraction level. For example, the color prediction at a pixel is independent from the color of the other pixels. Ignoring spatial correlation, the transform accuracy can be high in some areas of an image and low in others. In this paper, we empirically studied the influence of CATs on the low level image content (which we call the spatial content) that are colors, edges, textures and homogeneous areas. Based on conclusions we made and inspired by the Sharp transform proposed earlier by Finlayson *et al*.(Finlayson et al., 1994), we propose new constraints and formulate the derivation of CAT as a variational problem. The resulting transform is compared to some existing transforms based on the von Kries theory. The next section is devoted to studying the CATs influence on image spatial information. In Section 3, we present a new proposed approach to derive a CAT. Experimental results are addressed in Section 4. The last section concludes this work with some valuable issues.

2 COMPUTATIONAL CHROMATIC ADAPTATION EFFECT ON THE IMAGE CONTENT

In this section, a series of tests are conducted allowing to understand the von Kries-based CATs effect on images spatial content. In our experiments, we pay particular attention to edges, texture and homogeneous areas. Texture is characterized by its form, coarseness and complexity while edges are characterized by their sharpness and orientation.

2.1 Test Data

The reliability of experiments on chromatic adaptation depends on the test data accuracy. In our experiments, the used images are built using the image formation model. For a surface with a reflectance function $R(\lambda)$ and an illuminant $E(\lambda)$, the discrete image formation model is given by:

$$X = C \sum_{\lambda=400}^{700} E(\lambda)R(\lambda)VWX(\lambda) \quad (2)$$

$$Y = C \sum_{\lambda=400}^{700} E(\lambda)R(\lambda)VWY(\lambda) \quad (3)$$

$$Z = C \sum_{\lambda=400}^{700} E(\lambda)R(\lambda)VWZ(\lambda). \quad (4)$$

Where,

- VWX, VWY and VWZ are considered as the VW sensor sensitivities (Finlayson et al., 1994).
- Reflectance images R, are taken from the G. Finlayson *et al.* collection (Finlayson et al., 2004). This collection consists of a set of reflectance images of everyday objects with high spatial and spectral resolutions.
- The incandescent illuminant A and daylight D65, which are experimental illuminant approved by the CIE (CEI, 1998), are used.
- The constant $C = 100 \Big/ \sum_{\lambda=400}^{700} E(\lambda)VWY(\lambda)$ is used for normalization, yielding a value of $Y = 100$ for a perfect diffuser, which means that the reflectance is equal to one for all wavelengths (Lee and Goodwin, 1997). The wavelengths are sampled by an increment of $10nm$ in the visible interval $[400, 700]nm$.

- Finally, to display the image, the sRGB space is used. This color space is proposed by Hewlett-Packard and Microsoft via the International Color Consortium ICC (Stokes et al., 1996).

Having the reflectance multispectral images R, various test images could be constructed, according to the image formation model, using different light sources E and VW sensors sensitivity.

2.2 Methodology

The aim now is to study the CATs effect on the image content (homogeneous area, edges and texture). To achieve that, the following steps are followed.

- Twenty-three reflectance images of various objects and two standard illuminant (illuminant "D65" and illuminant "A") are used to construct test images using the image formation model as explained before. Altogether, there are 46 test images categorized in groups, which we will call groupA and groupD65.
- Consider a pair of images of the same scene taken under the standard illuminant "D65" and "A". The aim is to transform the test image under "D65" to the estimated image under "A" by using the von Kries based CATs. According to our experimentation, we found that the Bradford transform (CAT_B) provides the smallest distortion of the estimated images. Consequently, in the remainder of this section we will present only the scores of CAT_B. Hence, a third set of images, groupD65A, is built from groupD65 by using CAT_B.
- To evaluate distortions on step edge pixels, we consider the edge magnitude and orientation. For this purpose, we compute the mean ν, the variance σ^2 and the phase θ of the gradient images as follows:

$$\nu = \frac{1}{N \times M} \sum_i \sum_j |||G(i,j)|| - ||G_{ref}(i,j)||| \quad (5)$$

$$\sigma^2 = \frac{1}{N \times M} \sum_i \sum_j (|||G(i,j)|| - ||G_{ref}(i,j)||| - \nu)^2 \quad (6)$$

$$\theta = \arccos \frac{G \cdot G_{ref}}{\|G\| \|G_{ref}\|} \quad (7)$$

where G and G_{ref} are the gradient vectors of the estimated and reference $N \times M$ images, respectively and $\cdot$ is the dot product. Note that, the gradient is estimated by using the first partial derivatives of Gaussian.

- To assess the CAT_B effect on texture, a quantitative evaluation requires to use texture descriptors that allow measuring deformation. For this purpose, we use nine descriptors estimated from four cooccurrence matrices, corresponding to displacements equal to one in directions 0, $\pi/4$, $\pi/3$, and $3\pi/2$. The computation rules for these descriptors can be found in (Haralick et al., 1973). The squared Euclidean distance between the texture descriptors of the estimated and reference images is used to measure the CAT_B effect.
- To quantify the distortion between the adapted and the reference image, S-CIELAB error prediction metric is considered. However, for complex scenes, it should be noted that the variation of CIELAB ΔE_{94} is greater than the variation of S-CIELAB ΔE_s(Aldaba et al., 2006), but the shape of both variations is similar. Hence, we propose to use the color difference formula CIELAB ΔE_{94} between the adapted and the reference image. The ΔE_{94} between two colors (L_1, a_1, b_1) and (L_2, a_2, b_2) is computed as follows (Green and MacDonald, 2002):

$$\Delta E_{94} = \left[\left(\frac{\Delta L}{k_L S_L} \right)^2 + \left(\frac{\Delta C_{ab}}{k_C S_C} \right)^2 + \left(\frac{\Delta H_{ab}}{k_H S_H} \right)^2 \right]^{\frac{1}{2}} \quad (8)$$

Where $\Delta L = L_1 - L_2$ stands for the luminosity, $\Delta C = C_1 - C_2$ the chroma and $\Delta H = \{(\Delta a)^2 + (\Delta b)^2 - (\Delta C)^2\}^{\frac{1}{2}}$ the hue.
$C_1 = \sqrt{a_1^2 + b_1^2}$, $C_2 = \sqrt{a_2^2 + b_2^2}$, $\Delta a = a_1 - a_2$, $\Delta b = b_1 - b_2$, $k_H = 1$, $S_L = 1$, $S_C = 1 + 0.045C$, $S_H = 1 + 0.015C$, $k_C = k_L = 1$.
Note that, a ΔE_{94} of 1.0 is the smallest color difference that the human eye can notice.

2.3 Experimental Results

For the quantitative evaluation of the adapted images, ΔE_{94} color difference is computed between original and adapted images by considering, all pixels, homogeneous area and edge pixels. Note that, for the caused distortion to both texture and edge areas, grey level images have been considered. Table 1 shows the mean of ΔE_{94} according to the image content. We can notice that, the metric value changes according to the image content; it is not the same for edge pixels, homogeneous areas and overall the image pixels. In fact, compared to all pixels, the estimated error from homogeneous area and edges is about 7% and 3% greater, respectively. Thus we conclude that, the chromatic adaptation influence depends on the image spatial content.

Table 1: Mean of ΔE_{94} metric for CAT_{Bdf} as a function of image content.

Image content	ΔE_{94}
All pixels of the image	1.487
Edge pixels	1.535
Homogeneous area pixels	1.589

Our purpose now is to detect which specific characteristics are affected in texture and edges (strength or orientation or both). For that, as explained in the methodology sub-section, separate deformation measurement was defined for each image content. Table 2 presents the absolute difference in gradient magnitude of the two groups of images, *groupA* and *groupD65A*, according to a certain threshold, which is a percentage of the maximum value of the gradient magnitude. Thus a threshold of 5% corresponds to 5% of the maximum value of the gradient magnitude in the difference image. We noticed that, for a threshold (Th) of 5, 27.473% of all the edge pixels provides a mean value of 1.183 and a variance value of 0.788; this is not negligible relatively to the min and the max values of gradient magnitude, which are 0.454 and 9.078, respectively. Furthermore, for a threshold of 10, the percentage of eligible edge pixels is 14.084%, with a mean value of 1.687 and the associated variance is 1, which is also significant. Based on the obtained values, we can notice that the mean and the variance values increase with the threshold, while the percentage of eligible edge pixels decreases. Thus, the chromatic adaptation transformation produces an image with less contrast than the reference image, since the difference in image edges is not negligible. As conclusion, edge strength is modified while applying a CAT.

Table 3 shows the mean and variance of the angle between the gradient vector of the two groups of images, according to a certain threshold Th. We notice a considerable deviation in the gradient. In fact, from the threshold 5 to 25, the mean of the deviation ranges from 9.9 to 6.13 degrees. This is significant considering the percentage of eligible gradient vectors which are between 36.85% and 6.85%. To summarize:

- While increasing the threshold value, both the mean and the variance of the absolute difference in magnitude of gradients increase. However, the percentage of eligible edge pixels decreases.
- The mean over the smallest and highest gradient magnitudes ratios show that, the CAT_B effect is stronger for details than it is for obvious edges.
- Both the mean error and variance of edge orientation decrease when the smallest gradient magnitude increases. Again, details are the most vulnerable.

Table 2: Mean and variance of in gradient magnitude of the two image groups, according to empirical threshold.

Th	ν	σ^2	Max grad	Min grad	% of edge pixels
5%	1.183	0.788	9.078	0.454	27.47
10%	1.687	1.000	9.078	0.908	14.08
15%	2.215	1.313	9.078	1.362	7.362
20%	2.875	1.773	9.078	1.816	3.644
25%	3.592	2.084	9.078	2.270	1.998

Table 3: Mean and variance of gradient angle between gradient vectors of the two image groups, according to empirical threshold.

Th	ν	σ^2	% of edge pixels
5%	9.90	0.23	36.85
10%	8.62	0.20	22.43
15%	7.54	0.25	14.64
20%	6.63	0.19	10.15
25%	6.13	0.17	6.85

Table 4: Texture characteristics for displacement equal to 1 in the direction 0°.

Features	Ref	Ad	Euclidean distance
Mean	15.248	14.762	0.486
Variance	52.115	50.544	1.571
Energy	0.031	0.030	0.001
Entropy	4.138	4.140	0.001
Contrast	2.086	2.238	0.152
Homogeneity	0.779	0.775	0.004
Correlation	51.073	49.426	1.647
Cluster Shade	1137.740	954.656	183.080
Cluster Prominence	73821.300	66636.700	7184.660

Obtained texture features using groupA and groupD65A image sets are tabulated on Table 4. The Euclidean distance is used to perform a one-to-one comparison of these characteristics computed on a reference image (Ref) and an adapted one (Ad). Notice that, the two features that undergo a significant change are the shade and the prominence. The variation in cluster shade implies that the image loses its symmetry. While change in prominence means that, the number of pixels having grey levels close to the mean changes.

To conclude, CAT_B depends on the image spatial content. Indeed, homogeneous areas colors are more distorted than edge areas colors. The orientation and magnitude of weak edges are more distorted than those of obvious edges. For texture, the shade and prominence are the most deformed. Hence, our aim in the next section is to propose a new CAT taking the image spatial contents into consideration.

3 SPATIAL COMPUTATIONAL CHROMATIC ADAPTATION

An image can be seen as the summation of several cues such as shading, shadow, blur, edges and textures originating from physical phenomena which are illumination, reflectance and sensor sensitivity. Based on observations we made in the previous section, we can reasonably assume that, the cues behave differently when a CAT is applied. One can derive a CAT for each cue. For example, a step edge CAT can be estimated and used to transform pixels having a high gradient magnitude. To estimate a CAT, we propose to revisit the variational formulation of Finlayson *et al*. (Finlayson et al., 1994) and include the image data $d(\lambda)$ in the new CAT constraints. In addition, the CAT must fulfil the following requirements:

- Preserving the sensor gamut: This requirement allows the preservation of the sensed set of colors. Reducing this set, implies a reinforcement of metamerism. Increasing it may lead to output colors that are not physically realizable on the sensor.
- Reducing the overlap between spectral sensitivity of colored sensors: As showed in (Finlayson et al., 1994), this requirement allows a better color constancy. It can be formalized as a sharpening problem of sensors spectral sensitivities. Unlike the formalism of Finlayson *et al*., the sharpening of one sensor sensitivity function is related to the sharpening of the other sensitivity functions of the same sensor.
- Having a positive sensor response to a given data: It has been shown that this constraint leads to more accurate CAT (Drew and Finlayson, 2000).
- Being insensitive to noise: Noise insensitivity is beneficial, especially, when the CAT is estimated from real samples that can be noisy. We wish that, the transform remains unchanged when changing the variance of a white noise image. However, the energy of a spectral sensitivity function increases with the white noise variance because it is equal to the variance of its response to the centred white noise. Consequently, the last requirement can be fulfilled by setting the energy of sensitivity functions to a constant.

More formally, we denote the original sensor sensitivity functions as $\{b_k(\lambda)\}_{k=1}^{3}$. The sharpening of this sensor through a linear transform provides new sensitivity functions noted $c_k(\lambda) = \beta_k B(\lambda)^t$, where $B(\lambda)$ is the original sensor sensitivity functions vector and β is the linear sharpening transform. In what follows, we will show how to estimate the sharpening transform in the case of the k^{th} sensitivity function. The same procedure is applied for the two other sensitivity functions. The response of the k^{th} sharpened sensitivity function to the data $d(\lambda)$ is given by:
$d(\lambda)c_k(\lambda) = d(\lambda)B(\lambda)^t\beta_k = D(\lambda)^t\beta_k$.
where β_k is the vector of sharpening coefficients. Let Γ be the entire visible interval; $\Gamma = \Omega_k \cup \Phi_k$, where Φ_k is the sharpening interval associated with the k^{th} sensitivity function. The above mentioned requirements are translated to:

- Preserving the new sensor Gamut by minimizing the difference between the responses to the input data of the original and the new sensitivity function, that is:
  $\min_{\beta_k} \int_{\Phi_k} (D(\lambda)^t\beta_k - d(\lambda)b_k(\lambda))^2 d\lambda$
- Reducing the overlap between spectral sensitivities by minimizing the contribution of the other spectral sensitivities within the sharpening interval Φ_k, that is:
  $\min_{\beta_k} \int_{\Phi_k} \sum_{j\neq k} (D_j(\lambda)^t\beta_j)^2 d\lambda$ and minimizing the spectral response outside the sharpening interval, that is:
  $\min_{\beta_k} \int_{\Omega_k} (D(\lambda)^t\beta_k)^2 d\lambda$
- Reaching a positive solution when $\min_{\beta_k} B(\lambda)^t\beta_k \geq 0, \ \forall\lambda \in \Gamma$
- Setting the filter energy to one ensuring a robustness of the sharpening transform to the additive white noise: $\int_{\Omega_k} (B(\lambda)^t\beta_k)^2 d\lambda = 1$

We will write the discrete version of the variational problem used to find the optimal β_k. The combination of the first, the second and the fourth requirement into a variational formulation by additive rule is straightforward. However, the positivity constraint is not in an integral form. We propose to use an interior point formulation, where a logarithm slack function ensuring positivity is used, (Forsgren et al., 2002). Let us assume that we have N images (or image areas) taken under different illuminant. We consider ρ and μ Lagrange multipliers and $\varepsilon > 0$ a barrier parameter of the slack variables $r_k(\lambda)$, assumed positive. Moreover, the importance of each of the above measures is not defined. One can use a weighted combination of these measures and estimate the weights. However, the number of unknowns increases and the estimation may be under conditioned. We then propose to use binary weights allowing to identify the relevance of each measure. Given the color triplets $\{d_n\}_{n=1}^{N}$ and $B(\lambda)$, the sharpening transform is estimated by minimizing the following objective function:

Table 5: The four transfer matrices obtained with the image content-based method.

a_1	a_2	*Matrix*	*CAT*
1	1	1.1160 −0.045 −0.071 −0.568 1.3970 0.1710 0.0290 0.0800 0.8910	CAT_{d11}
0	1	1.1260 −0.060 −0.066 −1.074 1.8470 0.2270 0.0180 0.0820 0.9000	CAT_{d01}
1	0	2.0250 −1.092 0.0670 −1.716 2.8450 −0.128 0.0440 −0.189 1.1450	CAT_{d10}
0	0	2.1590 −1.206 0.0470 −1.094 2.1610 0.0670 0.0270 −0.201 1.1740	CAT_{d00}

$$
\begin{aligned}
\Psi_k(\beta,\mu) \quad = \quad & a_1 \sum_{n=1}^{N} \sum_{i\in\Phi_k} (D^n(\lambda_i)^t \beta_k - \\
& d^n(\lambda_i) b_k(\lambda_i))^2 \delta\lambda + \\
& a_2 \sum_{n=1}^{N} \sum_{i\in\Phi_k} \sum_{j\neq k} (D^n_j(\lambda_i)^t \beta_j)^2 \delta\lambda + \\
& \sum_{n=1}^{N} \sum_{i\in\Omega_k} (D^n(\lambda_i)^t \beta_k)^2 \delta\lambda + \\
& \rho(\sum_{i\in\Gamma} (B(\lambda_i)^t \beta_k)^2 \delta\lambda - 1) + \\
& \sum_{i\in\Gamma} \mu_i (B(\lambda_i)^t \beta_k - r_k(\lambda_i)) \delta\lambda - \qquad (9) \\
& \varepsilon \sum_{i\in\Gamma} log(r_k(\lambda_i)) \delta\lambda
\end{aligned}
$$

where $D^n(\lambda) = d^n(\lambda)B(\lambda)$ and $a_1 and a_2$ are the weighting parameters that have been added to select the best requirements. The above equations are solved by using the Newton method to determine β_k, the Lagrange multipliers μ, ρ, and ε as well as the slack function $r_k(\lambda)$. Note that, the earlier formulation provided by Finlayson *et al.* can be obtained by setting $a_1 = a_2 = 0$, $\rho = 1$, $\varepsilon = 0$, $\mu = 0$, and $d_n(\lambda) = 1$. The formulation with the positivity constraint described in (Drew and Finlayson, 2000) can be obtained by setting $a_1 = a_2 = 0$, $\rho = 1$ and $d_n(\lambda) = 1$. In addition, the transformation of an image under illuminant a to an other illuminant b is given by $\beta^{-1} D^{a,b} \beta$, where $D^{a,b}$ is the von Kries diagonal matrix, and β is the sharpening matrix where the columns are $\{\beta_k\}_{k=1}^{3}$. By resolving the above equation, four transformation matrices are obtained by combining coefficients a_1 and a_2 which may be 0 or 1 (Table 5).

Figure 1A depicts the VW sensors and the four new sensors, obtained by combining both coefficients a_1 and a_2. Note that, the combination $a_1 = a_2 = 0$ corresponds to the sharp transform of Finlayson *et al.* According to this figure, two cases are distinguishable, depending on whether coefficient a_1 is 0 or 1. In the first case (i.e., $a_1 = 0$), the resulting sensors are narrower and have greater amplitudes compared to the *VW* sensor. In the second case, in contrast, the sensors are larger and their amplitude is smaller than that of the *VW* sensor. Another significant remark relates to the negative values of the spectral distributions of the sharpened sensors, which are due to negative values of the calculated transfer matrices. This can cause color saturation problems during the imaging process.

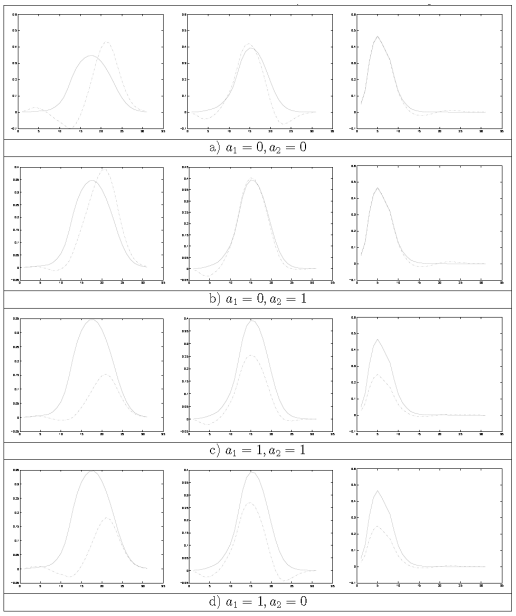

Figure 1: The new sensors in dotted lines compared to the *VW* sensor in solid line for each transfer matrix obtained by the proposed approach.

4 EXPERIMENTAL RESULTS

In this section, we aim to evaluate the four proposed chromatic adaptation transforms performance. First, we start by producing test images under illuminants A and D65. Example of test images are depicted in figures 2 and 3. Then, we change the illuminant of images under D65 toward illuminant A using various *CAT s* (proposed and existing). The comparison is carried out between test images generated using the image formation model under illuminant A (ground truth) and the adapted ones using different *CAT s*. This comparison is achieved following two evaluation criteria. The first one is related to the perceptual degradation assessment using the color difference metric presented earlier called ΔE_{94}. The second one is intended to measure the *CAT′s* effect on the image contents defined by edges and texture properties.

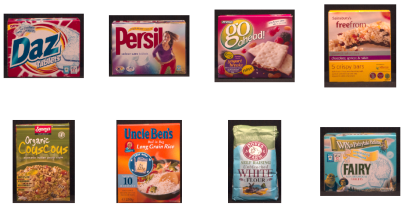

Figure 2: Examples of test images under illuminant D65.

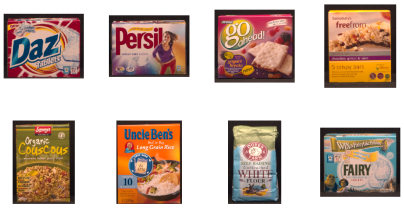

Figure 3: Examples of test images under illuminant A.

Figure 4: "Freeform" images obtained with the different CAT transforms, under illuminant A.

Figure 4, illustrates one example of corresponding images obtained by various *CAT s* on *Freeform* image.

4.1 Colorimetric Evaluation

$CIE\Delta E_{94}$ color difference is used, in *Lab* space, to estimate the perceptual color difference between the ground truth and the adapted image. It calculates an ellipsoid tolerance around the target color, such that the color belonging to this ellipsoid will be considered identical. This metric is recommended by *CIE* for the color difference quantification. Computed ΔE_{94} on obtained images illustrated in Figure 4 are tabulated on Table 6. We can notice that, the transformations $CATBradford$(CAT_B), CAT_{d11}, CAT_{d10} in that order provide the best results in terms of perception. However, the $CATSharp(CAT_S)$ quantitative evaluation is less acceptable. From ΔE_{94} metric stand of point, a ΔE_{94} value less than or equal to four is considered to be satisfactory (CEI, 2004).
Thus we conclude that, the proposed image content based transform CAT_{C11} provides more accurate performance compared to both $CATVonKries(CAT_V)$ and CAT_S. Furthermore, a competitive performance are noticed against CAT_B.

4.2 Content-based Evaluation

This evaluation involves calculating some characteristics related to the image content (edges and texture area) as explained previously. The considered characteristics are computed on the adapted images using the proposed CATs and the considered existing ones (Sharp, Von Kries and Bradford transforms). Then, the error is quantified using some specific criteria.

Edge Evaluation
We compute the edge map of the adapted and the ground truth images. The comparison concerns edges strength and orientation, as explained previously. Tables 7, 8 and 9 present the mean and the variance of the absolute difference between the gradient magnitude of the adapted and the reference images, for each transformation. Each table is related to a given threshold. This threshold stands for the percentage of a gradient magnitudes maximum. It is especially used to assess the significance of the gradient magnitude difference, which can be manifested as a difference in contrast between two image groups. Table 7 presents the obtained results for a threshold of 5% of the maximum value of the gradient magnitude difference in images. It can be seen that, the CAT_B transform performs better than the other transformations in terms of mean values. We note that, Compared to CAT_B, the CAT_{d11} transform obtains very close results in terms of mean value and performs better in terms of variance value and maximum magnitude value. Concerning Tables 8 and 9 which list the results for larger thresholds, namely 15% and 25%, the CAT_{d11} transform obtains the best results in term of mean, variance and maximum value. All in all, the proposed content-based transform performs slightly better than the others in preserving image edges.
Table 10 shows the mean and the variance values of the angle between the gradient vectors of the two image groups for each transformation. The CAT_{d11} gradient vector deviation is about 3.431 degrees compared to 6.551 and 8.68 degrees for CAT_B and CAT_S, respectively. According to these results we can argue that, the proposed CAT_{d11} provides the best performance in terms of edge pixels orientation preservation.
Texture Evaluation
We compare the texture descriptors of the reference and the adapted images as explained in the previous section. Table 11, shows the Euclidean distance of

Table 6: Computed color error on images of Figure 4.

	CAT_B	CAT_V	CAT_S	CAT_{10}	CAT_{d10}	CAT_{d11}
ΔE_{94}	1.487	2.285	6.377	2.438	2.080	1.92

Table 7: Mean and variance of the absolute difference in gradient magnitude between the ground truth and the adapted images for threshold equal to 5%.

	v	σ^2	Max grad	Min grad	% of edges pixels
CAT_S	6.160	21.427	40.083	2.004	23.52
CAT_{d01}	1.978	2.242	12.347	0.617	35.28
CAT_{d10}	1.449	1.585	10.085	0.504	23.99
CAT_{d11}	1.148	0.673	8.989	0.449	29.77
CAT_V	1.804	1.590	11.583	0.579	28.76
CAT_B	1.183	0.788	9.078	0.454	27.47

Table 8: Mean and variance of the absolute difference in gradient magnitude between the ground truth and the adapted images for a threshold of 15%.

	v	σ^2	Max grad	Min grad	% of edges pixels
CAT_S	11.222	21.152	40.083	6.013	8.07
CAT_{d01}	3.362	2.500	12.644	1.897	14.52
CAT_{d10}	3.940	3.3860	13.254	1.988	15.26
CAT_{d11}	2.072	1.054	8.988	1.349	9.53
CAT_V	3.070	1.483	11.583	0.738	10.82
CAT_B	2.215	1.313	9.078	0.362	7.362

the texture features, for each transformation matrix. An ordered ranking of the transformations according to the number of texture features where they perform, provides (in descending order): CAT_{d11}, CAT_B, CAT_{d10}, CAT_{d01}, CAT_V and CAT_S. Thus, CAT_{d11} is more accurate in terms of texture mean, contrast, homogeneity. Especially, cluster shade and cluster prominence which are the most affected texture properties according to the previous section. That means that, these properties are better preserved by the proposed CAT_{d11}.

5 CONCLUSION

This paper presents a new chromatic adaptation transforms transform (CAT) by considering the content information of a given image. Two main contributions are proposed. First, the authors prove that the chromatic adaptation transform affects differently the image contents, especially edges and texture area which are two essential elements in the human visual system. Second, the authors propose a new reformulation of chromatic adaptation transform (CAT) that considers the image content information. To achieve the first purpose, some well knowns $CAT s$ are considered. According to a perceptual color difference metric, results prove that these transforms depend on the image spatial content. Indeed, the homogeneous area colors are more distorted than those of edge areas. Furthermore, edge orientation and magnitude of weak edges are more distorted than those of obvious edges. For texture, the shade and prominence features are the most deformed features. Based on these conclusions, the authors reformulate the sharp transform considering new $CAT's$ requirements. From the variational formulation, four transforms have been proposed. Their performances are quantitatively evaluated against some well known transforms (Sharp, Bradford and von Kries). Experimental results showed that one of these transforms, namely CAT_{d11}, preserves better edges and texture features than the considered existing $CAT s$. Thus, taking the image content into account, to derive $CAT s$, can improve the preservation of both the color and the spatial content of the adapted images. Future works will involve the consideration of a large database and especially noisy data. In addition, the authors prospect to use other evaluation criteria.

Table 9: Mean and variance of the absolute difference in gradient magnitude between the ground truth and the adapted images for a threshold of 25%.

	v	σ^2	Max grad	Min grad	% of edges pixels
CAT_S	13.249	18.226	40.083	8.017	5.47
CAT_{d01}	3.982	2.690	12.644	2.529	9.5
CAT_{d10}	4.665	3.839	13.254	2.651	10.58
CAT_{d11}	2.689	1.618	8.988	2.247	4.31
CAT_V	3.658	1.320	11.583	2.317	6.96
CAT_B	2.875	1.773	9.078	2.27	3.64

Table 10: Mean and variance of absolute difference in gradient angle between the the ground truth and the adapted images for a threshold of 5%.

	v	σ^2	% of edge pixels
CAT_S	8.680	0.685	23.52
CAT_{d01}	5.574	0.197	35.28
CAT_{d10}	5.913	0.268	23.99
CAT_{d11}	3.431	0.160	29.77
CAT_V	7.249	0.365	28.76
CAT_B	6.551	0.384	27.47

Table 11: The Euclidean distance of texture features for each CAT.

Features	CAT_S	CAT_{d01}	CAT_{d10}	CAT_{d11}	CAT_B	CAT_V
Mean	0.336	0.283	0.152	0.070	0.174	0.486
Variance	5.993	0.687	0.592	0.462	0.308	1.571
Energy	0.002	0.001	0.001	0.001	0.001	0.001
Entropy	0.107	0.011	0.042	0.006	0.011	0.001
Contrast	0.213	0.106	0.027	0.071	0.072	0.152
Homogeneity	0.022	0.004	0.006	0.000	0.002	0.004
Correlation	5.384	0.740	0.605	0.426	0.343	1.647
Shade	279.2	112.6	77.8	59.61	68.35	183.0
Prominence	10330	4044	2825	900.5	2526	7184

REFERENCES

Aldaba, M. A., Linhares, J. M., Pinto, P. D., Nascimento, S. M., and K. Amano, D. H. F. (2006). Visual sensitivity to color errors in images of natural scenes. In *Visual Neuroscience, 23:555-559.*

Bianco, S. and Schettini, R. (2010). Two new von kries based chromatic adaptation transforms found by nu-

merical optimization. In *Color Research and Application, 35(3):184-192,*.

Bourbakis, N., Kakumanu, P., Makrogiannis, S., Bryll, R., and Panchanathan, S. (2007). Neural network approach for image chromatic adaptation for skin color detection. In *Int. Journal of Neural Systems, 17(1):1-12*.

CEI (1998). Commission internationale de l'eclairage. interim colour appearance model (simple version, ciecam97s). In *Technical Report, 131*.

CEI (2004). Commission internationale de l'eclairage. a review of chromatic adaptation transforms. technical report, 160. In *Visual Neuroscience*.

Drew, M. S. and Finlayson, G. (2000). Spectral sharpening with positivity. In *J. Opt. Soc. Am. A, 17:1361-1370,*.

Fairchild, M. D. (2005). Color appearance models. In *Second Edition, Wiley*.

Finlayson, G., Drew, M., and Funt, B. (1994). Spectral sharpening: Sensor transformations for improved color constancy. In *J. Opt. Soc. Am. A, 11(5):1553-1563*.

Finlayson, G., Hordley, S., and Morovic, P. (2004). A multispectral image database and an application to image rendering across illumination. In *Int. Conf. on Image and Graphics, 8-20, Hong Kong*.

Forsgren, A., Gill, P., and Wright, M. (2002). Interior methods for nonlinear optimization. In *SIAM Rev, 44:525-597*.

Gortler, S. J., Chong, H. Y., and Zickler, T. (2007). The von kries hypothesis and a basis for color constancy. In *ICCV, 1-8*.

Green, P. and MacDonald, L. (2002). Colour engineering: Achieving device independent colour. In *Wiley*.

Haralick, R., Shanmugan, K., and Dinstein, I. (1973). Textural features for image classification. In *IEEE Transactions on Systems, Man, and Cybernetics, 6(3):610-621,*.

Hirakawa, K. and Parks, T. W. (2005). Chromatic adaptation and white-balance problem. In *IEEE ICIP, 984-987*.

Holm, J., Susstrunk, S., and Finlayson, G. (2010). Chromatic adaptation performance of different rgb sensors. In *SPIE, 172-183*.

Kries, J. V. (1970). Chromatic adaptation. In *In D.L. MacAdam, (ed.) Sources of Color Science, The MIT Press, Cambridge MA, 120-127*.

Laine, J. and Saarelma, H. (2000). Illumination-based color balance adjustments. In *Color Imaging Conference: Color Science, Engineering Systems, Technologies and Applications, 202-206*.

Lam, K. M. (1985). Metamerism and colour constancy. In *Ph.D. Thesis, University of Bradford*.

Lee, H. C. and Goodwin, R. M. (1997). Colors as seen by humans and machinesy. In *Recent Progress in Color Science, 18-22*.

Luo, R. (2000). Color constancy: a biological model and its application for still and video images. In *Coloration Technology, 30:77-92*.

Madin, A. and Ziou, D. (2014). Color constancy for visual compensation of projector displayed image. In *Displays 35, 617*.

Spitzer, H. and Semo, S. (2002). Color constancy: a biological model and its application for still and video images. In *Pattern Recognition, 35:1645-1659*.

Stokes, M., Anderson, M., Shandrasekar, S., and Motta, R. (1996). A standard default color space for the internet - srgb. In *Version 1.10*.

West, G. and Brill., M. H. (1982). Necessary and sufficient conditions for von kries chromatic adaptation to give colour constancy. In *J. Math. Biol, 15:249-258*.

Wilkie, A. and Weidlich, A. (2009). A robust illumination estimate for chromatic adaptation in rendered images. In *Eurographics Symposium on Rendering*.